5 BURKE, G. J., and POGGIO, A. J.: 'Numerical electromagnetics code (NEC)—method of moments'. Technical document 116, Naval Ocean Systems Centre, San Diego, CA, 1981

6 ALTSHULER, E. E.: 'The travelling-wave linear antenna', *IRE Trans.*, 1961, **AP-9**, pp. 324–329

DIELECTRIC SLAB MATCHED FERRITE GYRATOR

Indexing terms: Dielectrics, Gyrators, Ferrite devices, Phase shifters

A 180° nonreciprocal ferrite phase shifter with stepped dielectric impedance transformer sections at both ends is designed using the method of field expansion into eigenmodes. The rigorous optimisation method includes the higher-order mode interaction between the step discontinuities. The design achieves compact and simple components, as relatively thick, and consequently short, uniform ferrite slabs of standard dimensions may be utilised. A computer-optimised design example provides about 180° ± 1° nonreciprocal differential phase shift between 12·2 and 12·8 GHz together with more than 24 dB return loss.

Introduction: Ferrite-slab loading of rectangular waveguides[1–7] is a well known technique for building simple nonreciprocal differential phase shifters for many applications. The gyrator with 180° phase difference is of considerable importance for composed components, e.g. for millimetre-wave circulators,[7,8] where compact design and good overall performance depend on the requirements that the individual parts are sufficiently short and have appropriate electrical characteristics. This letter presents a modal *S*-matrix method for designing compact ferrite slab gyrators with multisection dielectric impedance transformers at both ends (Fig. 1). The advantages are such that relatively thick, and consequently short, ferrite slabs may be utilised, that only a short DC magnetic field section is required, and that good VSWR and phase shift characteristics may be obtained by appropriate computer optimisation of all relevant parameters.

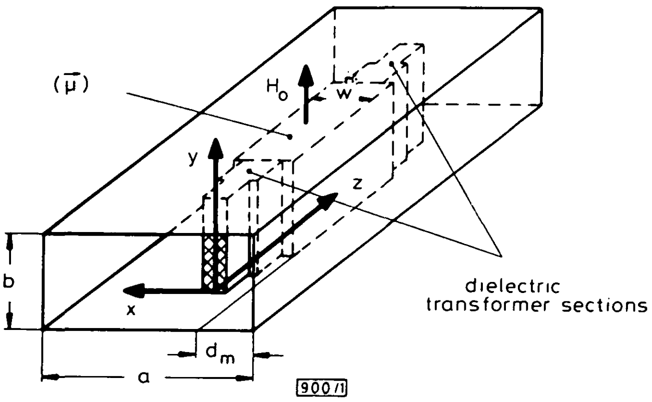

Fig. 1 *Ferrite-loaded waveguide gyrator with a uniform ferrite slab and multisection dielectric slab impedance transformers at both ends*

Many analyses of ferrite-loaded waveguides have previously been reported.[1–7] These investigations, however, are mostly restricted to uniform slabs. As for dielectric phase shifters,[9] the theory necessary for a rigorous treatment of the nonuniform structure of Fig. 1 should take into account the higher-order mode coupling effects at all discontinuities. The method for the computer optimisation given in this letter, which is based on field expansion into normalised incident and scattered waves, meets this requirement and yields directly the overall scattering matrix along the stepped structure.

Theory: The field

$$\nabla \times \vec{H} = j\omega\varepsilon\vec{E} \qquad \nabla \cdot (\langle\bar{\mu}\rangle\vec{H}) = 0$$
$$\nabla \times \vec{E} = -j\omega\langle\bar{\mu}\rangle\vec{H} \qquad \nabla \cdot \vec{E} = 0 \tag{1}$$

in each homogeneous subregion of the ferrite slab cross-section (Fig. 1) is derived from the electric field component $E_y \cdot \vec{e}_y$, which may be expressed as a sum of N eigenmodes[5,9] satisfying the vector Helmholtz equation and the boundary conditions at the metallic sidewalls:

$$E_y = \sum_{n=1}^{N} \begin{cases} E_n^{(r)} \sin\left[k_{xn}^{(r)}\left(x + d + \frac{w}{2}\right)\right] \\ E_n^{(m)} \sin(k_{xn}^{(m)}x) + F^{(m)} \cos(k_{xn}^{(m)}x) \\ E_n^{(l)} \sin\left[k_{xn}^{(l)}\left(a - d - \frac{w}{2} - x\right)\right] \end{cases} \tag{2}$$

where (r, m, l) denote the right, middle and left subregions across the ferrite-loaded waveguide section, respectively, d and w are the distance and width of the ferrite slab, respectively, and a z-dependence of $\exp(-\gamma_n z)$ is understood. For a DC magnetic field in the y-direction the permeability tensor takes the form[1]

$$\langle\bar{\mu}\rangle = \mu_0 \begin{bmatrix} \mu_1 & 0 & -j\kappa \\ 0 & \mu_r & 0 \\ j\kappa & 0 & \mu_1 \end{bmatrix} \tag{3}$$

with elements μ_1, μ_r, $j\kappa$ given in Reference 1. The propagation factors γ_n are determined via field matching[2,9] along the ferrite slab boundaries $x = \pm w/2$, and using the relations for the wavenumbers in eqn. 2. The requirement of the system determinant to be zero results in a transcendental equation for γ_n, which is solved numerically; see Reference 9.

For calculating the modal scattering matrix (S) of the step discontinuity waveguide to ferrite loaded waveguide, the related biorthogonality relations[2] for anisotropic structures have to be taken into account. Matching of the transversal field components at the corresponding interfaces at z = constant yields the relation between the still unknown amplitude coefficients through

$$(B) = (S)(A) \tag{4}$$

with the wave amplitude vectors A and B of the incident and reflected waves, respectively.

The series of steps is calculated by direct combination of the single scattering matrices, as in Reference 9, the lengths of the intermediate homogeneous rectangular waveguide sections being reduced to zero, if dielectric or ferrite slab-loaded structures are jointed together directly. For computer optimisation the expansion into 10 eigenmodes at each discontinuity has

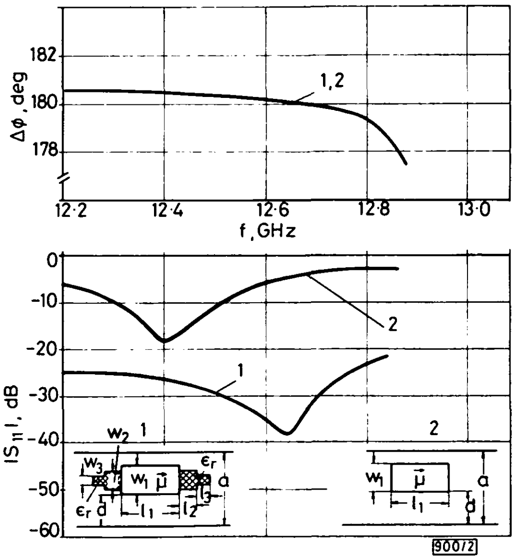

Fig. 2 *Optimised gyrator with two-step dielectric impedance transformers*

Nonreciprocal differential phase shift and input reflection coefficient in decibels as a function of frequency. Ferrite TTVG-1200 slab within R140 waveguide (15·799 mm × 7·899 mm). Dielectric material: D-13 (Trans. Tech. Inc.). Curve 1 with impedance transformers; curve 2 without impedance transformers. Design data: l_1 = 57·8 mm, w_1 = 1·2 mm, d = 13·55 mm, $H_0 = 1{\cdot}2 \times 10^5\,\mathrm{Am^{-1}}$, $\varepsilon_{fe} = 14{\cdot}5 - j0{\cdot}005$, $\varepsilon_{di} = 13 - j0{\cdot}003$, l_2 = 7·9 mm, w_2 = 0·98 mm, l_3 = 9·6 mm, w_3 = 0·76 mm turned out to yield sufficiently convergent behaviour. The final design data are proven through an expansion into 30 eigenmodes.

Results: A computer-optimised ferrite 180° phase shifter ('gyrator') using R140 waveguide housing dimensions (15·799 mm × 7·899 mm) has been chosen for a design example (Fig. 2). The uniform ferrite slab consists of standard TTVG-1200 ferrite material of width 1·2 mm, and the dielectric impedance transformer sections at both ends may be fabricated utilising D-13 material (Trans. Tech. Inc.) with a permittivity of $\varepsilon_r = 13$. To verify the improvement in the VSWR behaviour by the dielectric transformer sections (curves 1), the corresponding uniform slab phase shifter behaviour is included in the presentation (curves 2).

Acknowledgment: The authors thank the German Research Society DFG for financial support of the investigations under contract no. Ar 138/6-1.

J. UHER
F. ARNDT
J. BORNEMANN

Microwave Department
University of Bremen
Kufsteiner Strasse NW1
D-2800 Bremen 33, W. Germany

6th February 1987

References

1 LAX, B. K. J., BUTTON, K. J., and ROTH, L. M.: 'Ferrite phase shifters in rectangular waveguide', *J. Appl. Phys.*, 1954, **25**, pp. 1413–1421
2 COLLIN, R. E.: 'Field theory of guided waves' (McGraw-Hill, New York, 1960), pp. 85, 174–179, 198–209, Chap. 6
3 BERNUES, F. J., and BOLLE, D. M.: 'The ferrite-loaded waveguide discontinuity problem', *IEEE Trans.*, 1974, **MTT-22**, pp. 1187–1193
4 SODHA, M. S., and SRIVASTAVA, N. C.: 'Differential phase shift at microwave frequencies using planar ferrites', *ibid.*, 1976, **MTT-24**, pp. 215–216
5 HOFFMANN, M.: 'Die Streumatrix von Rechteckhohlleitungen mit magnetisierten Ferriteinsätzen endlicher Länge', *Arch. Elektron. & Übertragungstech.*, 1978, **32**, pp. 62–68
6 CHALOUPKA, H.: 'A coupled-line model for the scattering by dielectric and ferrimagnetic obstacles in waveguides', *ibid.*, 1980, **34**, pp. 145–151
7 GARDIOL, F. E.: 'Introduction to microwaves' (Artech House, Dedham, MA, 1981), Chap. 6.7
8 WALKER, P. W.: 'High-power mm-wave circulators and isolators designed to operate at 44 GHz', *Microwave Syst. News*, Dec. 1985, **15**, pp. 101–106
9 ARNDT, F., BORNEMANN, J., and VAHLDIECK, R.: 'Design of multisection impedance-matched dielectric-slab filled waveguide phase shifters', *IEEE Trans.*, 1984, **MTT-32**, pp. 34–38

LOW-LOSS DISPERSION-SHIFTED POLARISATION-MAINTAINING FIBRES

Indexing terms: Optical fibres, Optical dispersion, Polarisation

Low-loss polarisation-maintaining fibres, with the zero dispersion wavelength shifted to 1·56 μm, have been fabricated. A minimum transmission loss of 0·27 dB/km and crosstalk of −22 dB over a length of 4·1 km, corresponding to $h = 1{\cdot}53 \times 10^{-6}\,\mathrm{m}^{-1}$, are achieved at the same wavelength.

Introduction: Coherent optical communications require low-loss and low-dispersion optical fibres. In addition, the polarisation state must be maintained over the entire length.[1] Recently, the transmission loss of polarisation-maintaining fibres has been reported to be similar to that of conventional single-mode fibres.[2] Furthermore, fabrication techniques for long-length polarisation-maintaining fibres have been established.[3] Therefore, dispersion-shifted (DS) polarisation-maintaining fibres operating in the 1·5 μm wavelength region are prime candidates for long-length and high-speed coherent optical communication systems with long repeater spacings.

This letter describes the fabrication and characteristics of low-loss and low-crosstalk DS-PANDA fibres.

Table 1 FIBRE PARAMETERS AND CHARACTERISTICS OF DISPERSION-SHIFTED PANDA FIBRE

Peak index difference Δ_p, %	0·83
Mode field diameter $2a_{mf}$, μm	8·2
Fibre diameter $2b$, μm	200
Normalised SAP distance r/a_{mf}	5·1
Normalised SAP diameter t/b	0·53
Effective cutoff wavelength λ_c, μm	0·87
Zero dispersion wavelength λ_0, μm	1·56
Modal birefringence	$4{\cdot}0 \times 10^{-4}$
Crosstalk, dB	−22
Length, km	4·1
Mode coupling coefficient h, m^{-1}	$1{\cdot}53 \times 10^{-6}$
Minimum loss, dB/km	0·27

Fibre parameters: The parameters for a fabricated DS-PANDA fibre are listed in Table 1. The fibre was made using the pit-in-jacket method. A synthesised preform was used with a 40 mm outer diameter. This was produced by the VAD technique. The core and cladding consisted of GeO_2-doped and pure silica glasses, respectively. The stress-applying parts (SAPs) consisted of B_2O_3-doped silica glass. A refractive-index profile of the fibre, where Δ is the relative index difference from the cladding index, is shown in Fig. 1. Measurements were carried out by the RNFP method. The core had a graded index profile. Matched cladding was used to eliminate leaky modes. The peak index difference Δ_p was 0·83%. The mode field diameter $2a_{mf}$ and fibre diameter $2b$ were designed to be 8·2 μm and 200 μm, respectively.

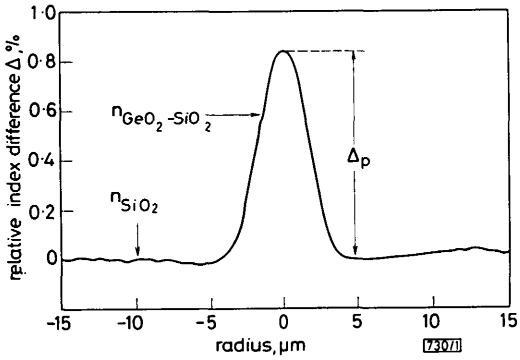

Fig. 1 *Refractive-index profile of dispersion-shifted PANDA fibre*

The SAP dopant concentration was 15 mol%. The normalised SAP distance r/a_{mf} was 5·1 and the normalised SAP diameter t/b was 0·5. The effective cutoff wavelength λ_c was measured as 0·87 μm. Modal birefringence of $4{\cdot}0 \times 10^{-4}$ was measured by the magneto-optic modulation method. The fibre was coated with silicone, resulting in a total diameter of 400 μm. The length of the fibre was 4·1 km.

Fibre characteristics: The experimental chromatic dispersion σ and group delay curves for the DS-PANDA fibre are shown in Fig. 2. The chromatic dispersion measurements were made

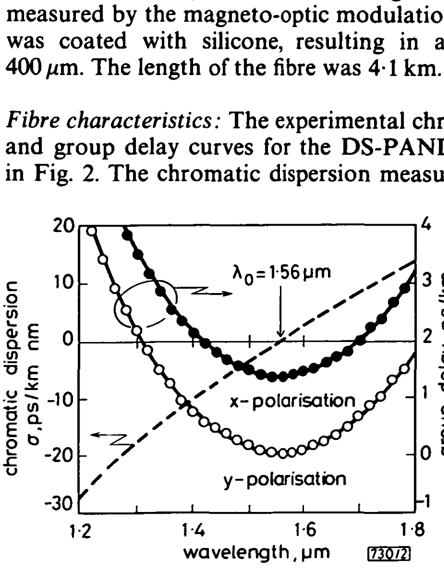

Fig. 2 *Chromatic dispersion for dispersion-shifted PANDA fibre*